Chapter 2

Ferroelectric Photovoltaic Effect

Rongli Gao, Zhenhua Wang, Chunlin Fu, Wei Cai, Gang Chen and Xiaoling Deng

Additional information is available at the end of the chapter

http://dx.doi.org/10.5772/intechopen.78238

Abstract

Tetragonal $BiFeO_3$ films with the thickness of 30 nm were grown epitaxially on (001) oriented $LaAlO_3$ substrate by using pulsed laser deposition (PLD). The transverse photovoltaic effects were studied as a function of the sample directions in-plane as well as the angle between the linearly polarized light and the plane of the sample along *X* and *Y* directions. The absorption onset and the direct band gap are ~2.25 and ~2.52 eV, respectively. The photocurrent depends not only on the sample directions in-plane but also on the angle between the linearly polarized light and the plane of the sample along *X* and *Y* directions. The results indicate that the bulk photovoltaic effect together with the depolarization field was ascribed to this phenomenon. Detailed analysis presents that the polarization direction is along [110] direction and this depolarization field induced photocurrent is equal to ~3.53 μA/cm^2. The BPV induced photocurrent can be approximate described as $Jx \approx 2.23\cos(2\theta)$, such an angular dependence of photocurrent is produced as a consequence of asymmetric microscopic processes of carriers such as excitation and recombination.

Keywords: transverse, photovoltaic effect, depolarization, tetragonal $BiFeO_3$, photocurrent

1. Introduction

Driven by the energy crisis all over the world, more and more researchers have begun to investigate a broad spectrum of candidate materials for thin-film photovoltaic cells as a renewable energy production [1–3]. Among them, ferroelectric photovoltaic effect has been received considerable attention in the past few years because of its potential application in optoelectronics, information storage and energy conversion [4, 5]. However, different mechanisms have been proposed to explain experimental observations in the literature, such as the

depolarization field effect [6–8], interface effect [9], domain theories [10], or spin polarization [11]. It is worth mentioning that bulk photovoltaic effect (BPVE) is another primary mechanism, which was discovered in noncentrosymmetric ferroelectrics several decades ago. It is often suggested that different from p-n junction based systems, BPVE does not require an asymmetric interface, especially its photovoltage is not limited by the band gap of the material, which can reach 10^3 V/cm or more and it is called anomalous photovoltaic effect [12–14]. All of the various ferroelectric materials, $BiFeO_3$ (BFO) is of particular interest because of its robust ferroelectricity, room temperature coexistence of ferroelectric and antiferromagnetic orders and the possible magnetoelectric couple effect. More important, the band gap of BFO (~2.7 eV) is smaller than many other ferroelectric materials (more than 3 eV), making it become a more suitable candidate materials for the next generational thin-film photovoltaic cells. Apart from the fundamental research on its ferroelectric properties, the photovoltaic effect of BFO has been reported in ceramics, nanowires, single crystals and highly oriented films [15–17]. However, in all of these studies, BFO is a rhombohedrally distorted perovskite [18] belonging to the *R*3*c* space group, each Fe^{3+} center is coordinated by six O^{2-} ions, although the distortion along [111] yields a quasioctahedral arrangement [19]. Since its photovoltaic tensor have a nonzero G_{22} component, photocurrent should exist in the direction perpendicular to the ferroelectric polarization [20]. Recently, first-principles calculations predicted that a metal stable tetragonal (T) phase with a giant axial ratio (~1.27) and an extremely large spontaneous polarization of P ~ 150 μC/cm² can be achieved in BFO under a compressive strain [19], which were confirmed by several experiments [21–23]. Besides, the first principles theoretical calculations predict a smaller band gap in tetragonal BFO than in rhombohedral one [19]. Therefore, it is a great importance to research the photovoltaic effects due to its smaller band gap and more larger polarization as well as its special directions. In this letter, we report on photovoltaic devices based on tetragonal BFO thin films that demonstrate bulk photovoltaic effect and represent an interesting alternative material class for study of mechanism of photovoltaic effect and in pursuit of energy related applications.

2. Experimental process

Tetragonal phase $BiFeO_3$ (T-BFO) films of ~30 nm thickness were fabricated epitaxially by pulsed laser deposition (PLD) technique on (001)-oriented $LaAlO_3$. In this experimental process, KrF excimer laser with the wavelength of 248 nm was used for deposition, the deposition frequency is 3 Hz with an energy of about 240 mJ. The substrate was kept at 650°C with 11 Pa of oxygen atmosphere. In the course of deposition, the substrate holder was still rotated with the speed of 360°/min so that the thickness variation of the film can be reduced and the uniform composition of the film can be obtained as much as possible. Followed the deposition, oxygen stoichiometric T-BFO films were in situ annealed in 500 Pa oxygen pressure and cooled slowly down at 5°C/min to room temperatures to avoid the effect of deficient oxygen. Structural characterization was performed using X-ray diffraction (XRD), using M/s Bruker make D8-Discover system. Room temperature transmittance and reflectance spectra were collected by using a Perkin-Elmer Lambda-900 spectrometer (with the energy of 0.41–6.53 eV). For the conductive characteristics measurements, platinum electrodes of 200 μm length and

interelectrode distances of 20 μm were fabricated by sputter deposition using conventional photolithography and lift-off technique. The photoelectric effect was measured by illuminating the gap between the electrodes with a $\lambda \approx 405$ nm ($E \approx 3.06$ eV) laser (Newport LQA405-85E) with a maximum power of 80 mW for the illumination, yielding the incident light power density on the sample surface up to 0.8 W/cm^2 and simultaneously measuring the photocurrent using a high-input impedance electrometer (Keithley 6517).

3. Results and discussion

Figure 1(a) shows the results of the X-ray diffraction θ–2θ scans of the T-BFO deposited on (001) LAO substrates. Only peaks corresponding to (00*l*) reflections of BFO and those from the substrate are seen, indicating the epitaxial growth of the films. The out-of-plane lattice parameter *c* calculated from the (00*l*) peaks is estimated to be ~4.67 Å, which is larger than that of rhombohedral BFO reported [14–16]. The larger lattice parameter c of T-BFO means that it is stabilized by a large compressive strain. The reciprocal-space map of BFO films indicates that the in plane parameter of BFO is very close to that of LAO, i.e., a ~ 3.79 Å and the BFO film with an out-of-plane lattice parameter of 4.67 Å were detected, indicating that the film is pure tetragonal-like. This corresponds to c/a ~ 1.27 for BFO in the sample. **Figure 1(b)** shows the topography of the corresponding film. The AFM image reveals a smooth surface morphology with a surface roughness of ~0.5 nm. In order to research the polarization direction, the planar Pt electrodes were patterned on the films to directly measure the in-plane P-E loops.

As shown schematically in **Figure 1(c)**, the edge of the Pt electrode was aligned along the [100] and [110] directions of the substrate, so as to ensure the electric field directions. The applied electric field *E* was determined using $E = V/d$, where *V* is the voltage and *d* is the channel width. **Figure 1(d)** shows the P-E hysteresis loop for the T-BFO films on LAO substrate when *E* is along the [100] and [110] directions, respectively. One can clearly see that hysteresis loop saturation in each direction is evident. The remnant polarization along the [100] and [110] directions are 30 and 37 μC/cm^2, respectively, consistent with previous study [24]. This different polarization in various directions should be attributed to the different polarization component. Besides, the coercive field along [110] is larger than that of [100] directions, this may be that the polarization in the [110] direction is more stable and domains wall pinning effect and grain boundary along different directions. It is noteworthy that the coercive field (E_c) along [110] is asymmetric in positive and negative position, which may be due to a residual strain in the crystal or might be the different internal field in each interface. The in-plane measure structure can be used to investigate the in-plane photovoltaic effect and strain effect of ferroelectric and multiferroic films.

The transmission spectrum of the samples were displayed in **Figure 2(a)**, the direct band gap is extracted by a linear extrapolation of an $(\alpha.E)^2 \sim E$ plot to zero, as shown in inset of **Figure 2(a)**. It is clear that the band gap in tetragonal $BiFeO_3$ is 2.52 eV, which is 0.13 eV smaller than that in rhombohedral $BiFeO_3$ (2.68 eV). This result is mainly consistent with the results from the theoretical calculations [19]. We have performed detailed photoelectric investigations on BFO epitaxial thin films with T-Phase to get a better insight into the actual

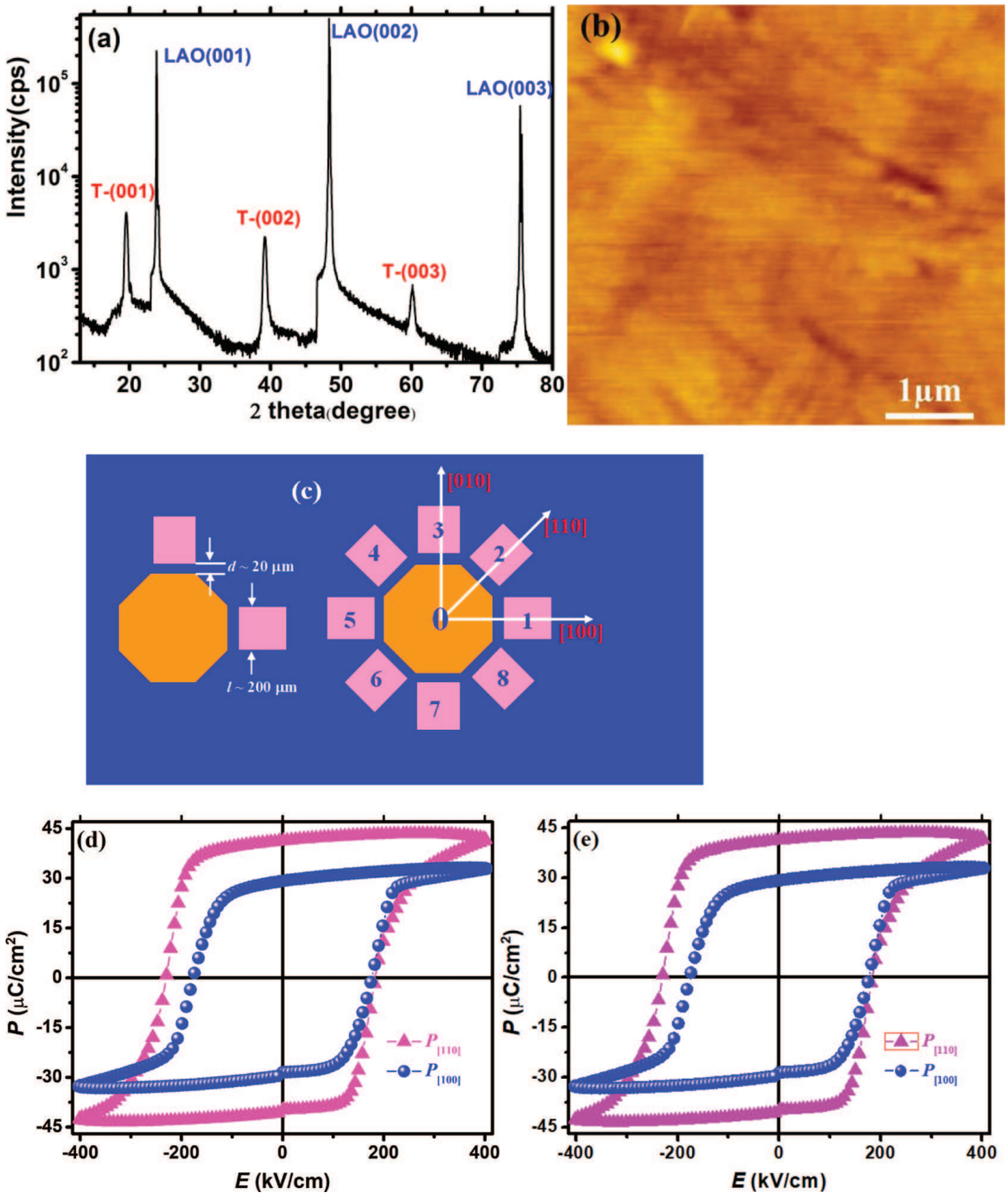

Figure 1. (a) XRD spectrum of tetragonal phase $BiFeO_3$ films grown on $LaAlO_3$ substrate. (b) The topography of the corresponding film by AFM. (c) Schematic illustration of the sample geometry used for the P-E curve measurements. (d) Field-dependent variation of P-E loops of the tetragonal $BiFeO_3$ films grown on $LaAlO_3$, and the applied electric field is along the [100] and [110] direction.

mechanism of ferroelectric photovoltaic effect. Pt in-plane electrodes with a gap of 20 μm were patterned by a standard photolithography process. The x axis is along the [100] direction and y axes is parallel to the [010] direction while z is perpendicular to both the y and x axes,

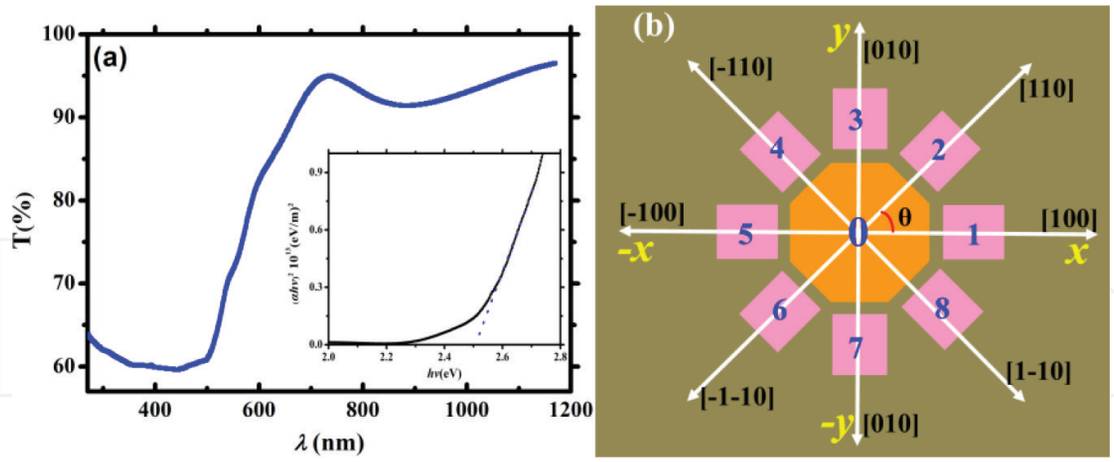

Figure 2. (a) Transmission spectrum of tetragonal $BiFeO_3$ films. Inset shows the direct band gap analysis. (b) Schematic illustration of the sample geometry used for the photocurrent measurements of the epitaxial tetragonal BFO thin film with in-plane electrodes. The angle between the polarizer transmission axis and the x axis is θ.

forming a right-hand coordinate system. The angle between the [100] direction (x axes) and the direction of current (I_{oc}) flow is θ, as shown in **Figure 2(b)**.

To measure the photovoltaic effect of T-BFO films, we illuminated the gap areas between the top Pt electrodes, unwanted light illumination on the surfaces was avoided by covering with black tape. In the process of measuring the photovoltaic effect, the central electrode was connected with the negative side of source meter (Keithley 6517) and the outer electrodes were linked to the positive one. The photocurrent density J was determined using $J = I/(d.t)$, where I is the measured short-circuit current voltage, d is the channel width and t is the film thickness, $J_{[hkl]}$ denotes the current flows along [hkl] direction, as shown in **Figure 2(b)**. **Figure 3(a)** shows time dependence of photocurrent density, showing a good retention of the photovoltaic effect, exhibiting no degradation when it was measured during several on-and-off cycles. The photocurrent density J along [100] direction ($J_{[100]}$ ~ 1.24 μA/cm^2) is always smaller than that of [110] direction ($J_{[110]}$ ~ 2.24 μA/cm^2), this distinct difference may be a result of a larger depolarization field along [110] direction compared with [100] direction due to the larger polarization along [110] direction, as shown in **Figure 1(d)**. From the P-E curves we can find that the polarization along (110) direction is larger than that of (001) and (010) directions, therefore we suppose that the component of polarization in the x-y plane should lie along the (110) direction. It was reported that photocurrent can be tuned by the depolarization field, i.e., different polarization will induce unlike photocurrent. Because the polarization along (110) direction is larger than that of (001) and (010) directions, thus, the depolarization filed along (110) direction is larger than that of (001) and (010) directions and so does the photocurrent. This result presents a evident influence of depolarization field on the transverse photovoltaic effects. To prove this viewpoint, we have reversed the polarization along the [100] and [110] directions to check the polarization dependence of photovoltaic effect. Both the photocurrent along [100] and [110] directions decrease after polarization switching, as shown in **Figure 3(b)**. This decreased photocurrent indicates that the photocurrent is at least composed of two parts, one is the contribution of depolarization field, another one will be discussed later.

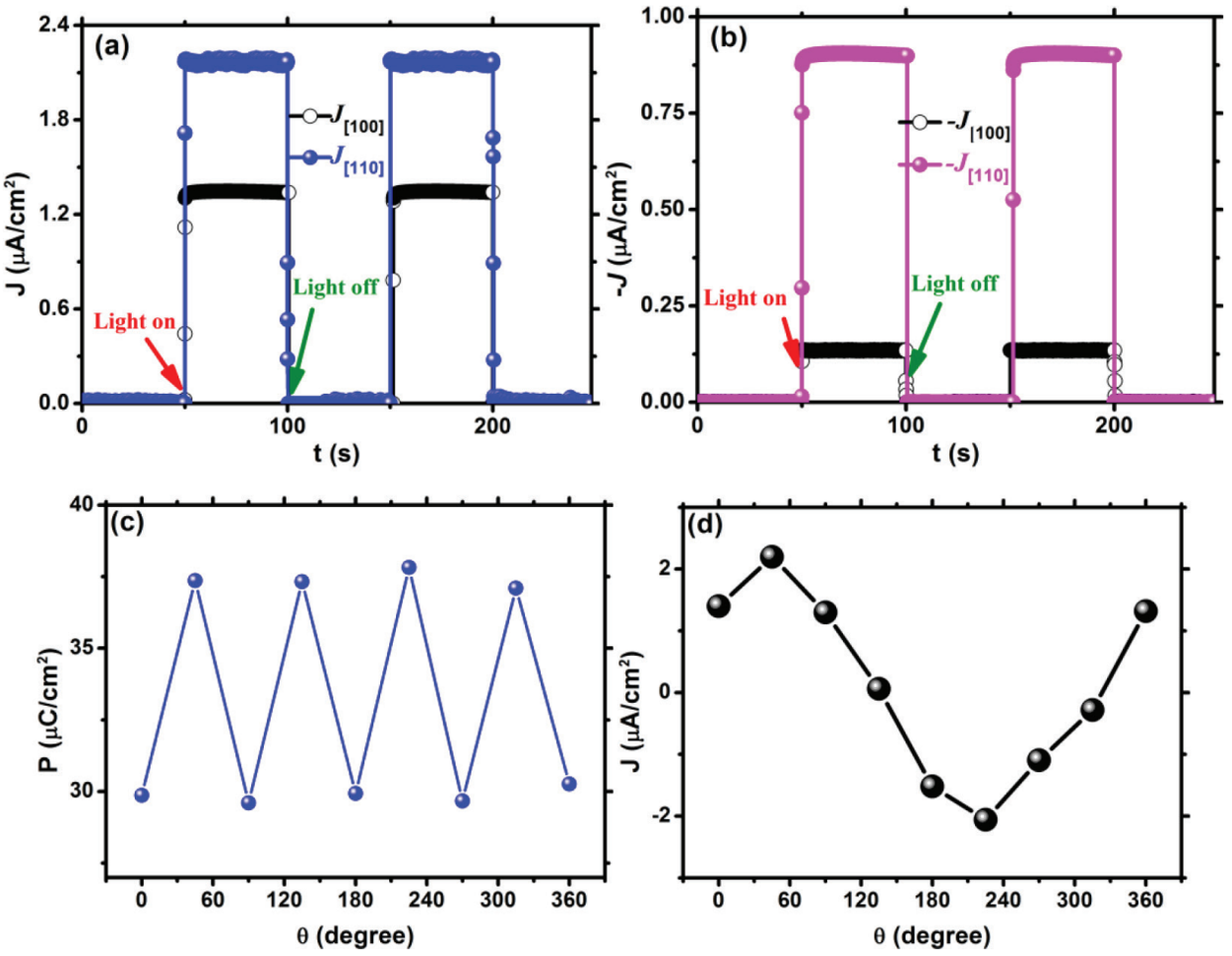

Figure 3. (a) Time dependence of short-circuit photocurrent for the $BiFeO_3$ samples with light on and off along [100] and [110] directions with the film is polarized by positive voltages. The negative electrode connected with point "0", i.e., the central electrode and the positive electrode connected with other points, i.e., the outer electrodes. (b) Time dependence of short-circuit photocurrent for the $BiFeO_3$ samples with light on and off along [100] and [110] directions with the film is polarized by negative voltages. (c) The angular dependence of polarizations. (d) Photocurrent as a function of crystal orientation.

In order to elucidate the crystallographic direction and polarization dependence of photocurrent, we measured the PV current by changing the angle between the [100] direction and the direction of current flow (*x* direction), i.e., measure the photocurrent and polarization along different directions, as shown in **Figure 3(c)** and **(d)**. We find that both the photocurrent and polarization along different directions show fluctuation behavior, more importantly than all of that, the absolute values of polarization along *x* and *y* axes are smaller than in other directions, while the photocurrent is a local maximum (~2.2 μA/cm²) parallel or antiparallel to [110] direction while the minimal value can be obtained when measured along [-110] or [1-10] directions. These results suggest that the different values of photocurrent along different crystallographic direction can be attributed to the inequality depolarization field and the minimum photocurrent occurs when it is perpendicular to the polarization directions. However, we found that the angular dependence of polarizations shows obvious difference from that of photocurrent, indicating that the photocurrent is not entirely decided by polarization, which presents typical bulk effect.

Therefore, our results mentioned above cannot be explained by the depolarization field effect simply. Such a crystallographic direction dependence can be described in the framework of the bulk photovoltaic (BPV) theory, where the photocurrent is produced as a consequence of asymmetric microscopic processes such as excitation and recombination of photon induced electrons and holes [25, 26]. According to this theory, the dependence of the photocurrent on the polarization orientation of incident light can be expressed by a bulk photovoltaic tensor. The BPV effect has been studied extensively, it is assumed that the photocurrent in non-centrosymmetric ferroelectrics materials depends on the orientation of the crystal with respect to the projections of the electric field of the linearly polarized light onto the plane of the sample along X and Y directions [26], when the light propagating along Z direction, the photocurrent generated along X and Y directions with can be expressed by [26–28].

$$J_x = -I\beta_{22}\sin 2\theta \text{ and } J_y = I\beta_{22}\cos 2\theta \tag{1}$$

where I, β_{22} and θ are the intensity of light, bulk photovoltaic tensor coefficient and the angle between the plane of the linearly polarized light and X direction.

In order to prove the existence of the BPV in our films, we measured the photo current for T-BFO films by changing the angle between the plane of the linearly polarized light and the direction of current flow (x direction). The schematic diagram of the experimental configuration was given in **Figure 4(a)**. The photo current was measured with the negative electrode connected with point "0", i.e., the central electrode and the positive electrode connected with outer electrodes. θ is defined as the angle between the linearly polarized light and the plane of the sample along x axes, i.e., the [100] direction. The photocurrent densities along and perpendicular [110] direction were measured at different polarizer angles for the samples, which is presented in **Figure 4**. It is clearly that the photocurrent exhibits definitive angular dependency, however, the magnitude and signs of the photocurrent varied with directions, i.e., the photocurrent is relatively smaller and the sign changes with angle when it perpendicular the [110] direction (that is, along [-110] or [1-10] directions), while it is larger and it is always a positive value since it is along [110] and [-1-10] directions. This result demonstrates that excepted for the BPV, other factors such as interfacial barrier, domain walls, depolarization field, as well as a misalignment between the light direction and the sample surface can contribute to the photocurrent. As a consequence, a constant current J_0 should be introduced to Eq. (1), which can be expressed as:

$$J_x = J_{x0} - I\beta_{22}\sin(2\theta + \theta_0) \text{ and } J_y = J_{y0} + I\beta_{22}\cos(2\theta + \theta_0) \tag{2}$$

For the above four directions, the results can be fitted very well to a cosine function. The fitting function is for the four directions as follows: $J_{[-110]} = -2.21\cos(2\theta - 13°)$, $J_{[1\text{-}10]} = -2.26\cos(2\theta - 12°)$, $J_{[110]} = -3.23 + 1.97\cos(2\theta - 9°)$, and $J_{[-1\text{-}10]} = 3.51 + 2.13\cos(2\theta - 11°)$, respectively. It is worth emphasizing again that the constant current J_0 is near zero for the [-110] and [1-10] directions, i.e., perpendicular the polarization direction ([110] direction), which shows typical bulk photovoltaic effect. However, the constant currents are −3.23 and 3.51 for [110] and [-1-10]

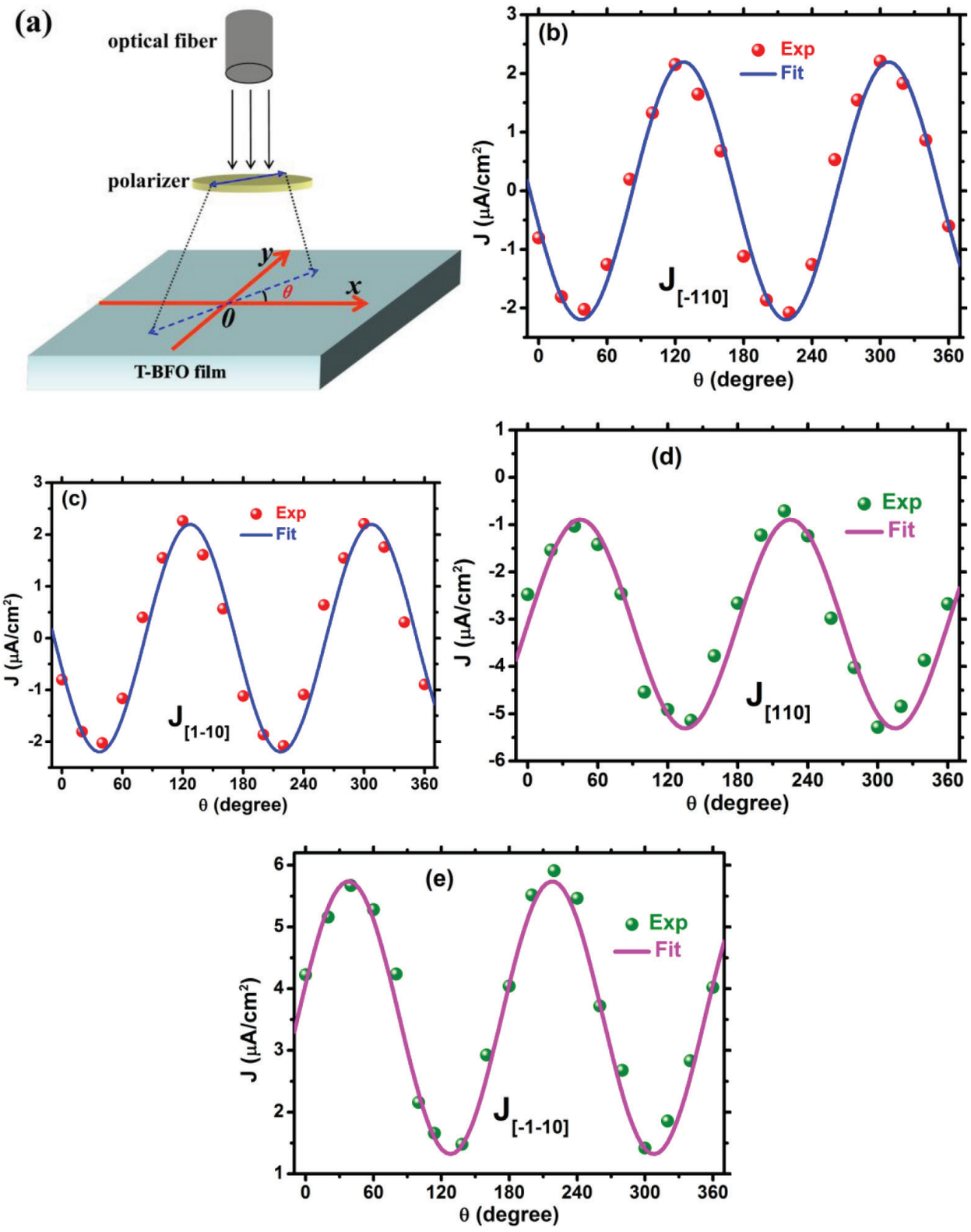

Figure 4. (a) The schematic diagram of the experimental configuration. The photocurrent was measured with the negative electrode connected with the central electrode and the positive electrode connected with the outer electrodes. θ is defined as the angle between the linearly polarized light and the plane of the sample along x axes, i.e., the (100) direction. Photocurrent measured at different angles, with the direction of the current flow along [-110] direction (b), [1-10] direction (c), [110] direction (d) and [-1-10] direction (f). The solid line represents the fit with Eq. (2).

directions, respectively. We argue that this different positive and negative constant current can be attributed to the depolarization field effect, different direction of depolarization field will lead to different photocurrent because the photocurrent is opposite to that of polarization direction according to depolarization theory [13]. Nonetheless, we note that the compensated angle θ is near the same and is very closer to zero, this very small compensated angle may be a result of the misalignment between the light beam direction and the normal to the sample surface while the constant current J_0 parallel to the [110] and [-1-10] directions should have been ascribed to the depolarization or the asymmetry interface barriers between the internal electrode and outer electrode. Combined the results of **Figures 3** and **4** with **Figure 1(e)**, we can deduce that although the polarization direction in the tetragonal phase BFO films lies nearly the (001) direction, a fraction of the component of polarization direction on the sample surface lies along the [110] direction. It should be emphasized that the photocurrent measured perpendicular to [110] direction is perpendicular to the ferroelectric polarization, hence, the results cannot be explained by the depolarization field. Moreover, The use of symmetric in-plane Pt electrodes can exclude the photovoltaic effect from the interfacial energy barriers mostly, and domain walls cannot explain the angular dependence of the photocurrent and thus they can be excluded here.

Therefore, the photovoltaic effect along [-110] and [1-10] directions are both perpendicular to [110] direction, which is a product of BPV, yet it is a total effects combined depolarization and BPV effects when the photocurrent measured parallel to [110] and [-1-10] directions. Based on above analysis, depolarization field induced photocurrent is equal to the constant current J_0 (~3.53 μA/cm^2). The BPV induced photocurrent can be approximate described as $Jx \approx 2.23\cos(2\theta)$, such an angular dependence of photocurrent is produced as a consequence of asymmetric microscopic processes of carriers such as excitation and recombination [5].

4. Conclusions

Tetragonal $BiFeO_3$ films with the thickness of 30 nm were grown epitaxially on (001) oriented $LaAlO_3$ substrate by using pulsed laser deposition (PLD) and the photovoltaic effect of tetragonal $BiFeO_3$ along different crystallographic direction with in plane symmetric electrodes was investigated, the absorption onset and the direct band gap are ~2.25 and ~2.52 eV, respectively. The photocurrent exhibits definitive angular and direction dependency, indicating obvious bulk photovoltaic effect and depolarization field effect. The photocurrent depends not only on the sample directions in-plane but also on the angle between the linearly polarized light and the plane of the sample along X and Y directions. The polarization direction is along [110] direction and the photocurrent induced by this depolarization field is as large as ~3.53 μA/cm^2, while the BPV induced photocurrent can be described as $Jx \approx 2.23\cos(2\theta)$, such an angular dependence of photocurrent is produced as a consequence of asymmetric microscopic processes of carriers such as excitation and recombination. These results indicate that the BPV and depolarization field effect in tetragonal $BiFeO_3$ thin films could be further explored for the next generation of solar photovoltaic applications.

Acknowledgements

This work is supported by the National Natural Science Foundation of China (51402031), the Program for Innovation Teams in University of Chongqing, China (Grant no. CXTDX201601032) and the Natural Science Foundation Project of Chongqing (CSTC2015jcyjA50015).

Author details

Rongli Gao[1,2]*, Zhenhua Wang[1,2], Chunlin Fu[1,2], Wei Cai[1,2], Gang Chen[1,2] and Xiaoling Deng[1,2]

*Address all correspondence to: gaorongli2008@163.com

1 School of Metallurgy and Materials Engineering, Chongqing University of Science and Technology, Chongqing, China

2 Chongqing Key Laboratory of Nano/Micro Composite Materials and Devices Chongqing, China

References

[1] Ginley D, Green MA, Collins R. Solar energy conversion toward 1 terawatt. MRS Bulletin. 2008;**33**:355

[2] Gur I, Fromer NA, Geier ML, Alivisatos AP. Air-stable all-inorganic nanocrystal solar cells processed from solution. Science. 2005;**310**:462

[3] O'Regan B, Grätzel M. Optical electrochemistry I: Steady-state spectroscopy of conduction-band electrons in a metal oxide semiconductor electrode. Nature London. 1991;**353**:737

[4] Fridkin VM, Popov BN. Anomalous photovoltaic effect in ferroelectrics. Soviet Physics Uspekhi. 1978;**21**:981

[5] Glass AM, von, der Linde D, Negran TJ. High-voltage bulk photovoltaic effect and the photorefractive process in $LiNbO_3$. Applied Physics Letters. 1974;**25**:233

[6] Glass AM, von, der Linde D, Auston DH, Negran TJ. Excited state polarization, bulk photovoltaic effect and the photorefractive effect in electrically polarized media. Journal of Electronic Materials. 1975;**4**:915

[7] Brody PS, Crowne F. Mechanism for the high voltage photovoltaic effect in ceramic ferroelectrics. Journal of Electronic Materials. 1975;**4**:955

[8] Nelson J. The Physics of Solar Cells. London: Imperial College Press; 2003

[9] Gregg BA. Excitonic solar cells. The Journal of Physical Chemistry B. 2003;**107**:4688

[10] Yang SY, Seidel J, Byrnes SJ, Shafer P, Yang C-H, Rossell MD, Yu P, Chu Y-H, Scott JF, Ager JW, III LWM, Ramesh R. Above-bandgap voltages from ferroelectric photovoltaic devices. Nature Nanotechnology. 2010;**5**:143-147

[11] Ganichev SD, Prettl W. Spin photocurrents in quantum wells. Journal of Physics: Condensed Matter. 2003;**15**:R935

[12] Basu SR, Martin LW, Chu Y-H, Gajek M, Ramesh R, Rai RC, Xu X, Musfeldt JL. Photoconductivity in $BiFeO_3$ thin films. Applied Physics Letters. 2008;**92**:091905

[13] Gao RL, Yang HW, Sun JR, Zhao YG, Shen BG. Oxygen vacancies induced switchable and nonswitchable photovoltaic effects in $Ag/Bi_{0.9}La_{0.1}FeO_3/La_{0.7}Sr_{0.3}MnO_3$ sandwiched capacitors. Applied Physics Letters. 2014;**104**:031906

[14] Wang J, Neaton JB, Zheng H, Nagarajan V, Ogale SB, Liu B, Viehland D, Vaithyanathan V, Schlom DG, Waghmare UV, Spaldin NA, Rabe KM, Wuttig M, Ramesh R. Epitaxial BiFeOmultiferroic thin film heterostructures. Science. 2003;**299**:1719

[15] Catalan G, Scott JF. Physics and Applications of Bismuth Ferrite. Advanced Materials. 2009;**21**:2463

[16] Li JF, Wang JL, Wutiig M, Ramesh R, Wang NG, Ruette B, Pyatakov AP, Zvezdin AK, Viehland D. Dramatically enhanced polarization in (001), (101), and (111) BiFeO3 thin films due to epitiaxial-induced transitions. Applied Physics Letters. 2004;**84**:5261

[17] Gao RL, Chen YS, Sun JR, Zhao YG, Li JB, Shen BG. Complex transport behavior accompanying domain switching in $La_{0.1}Bi_{0.9}FeO_3$ sandwiched capacitors. Applied Physics Letters. 2012;**101**:152901

[18] Fischer P, Polomska M, Sosnowska I, Szymanskig M. Temperature dependence of the crystal and magnetic structures of $BiFeO_3$. Journal of Physics C. 1980;**13**:1931

[19] Tütüncü HM, Srivastava GP. Electronic structure and lattice dynamical properties of different tetragonal phases of $BiFeO_3$. Physical Review B. 2008;**78**:235209

[20] Fridkin VM. Bulk photovoltaic effect in noncentrosymmetric crystals. Crystallography Reports. 2001;**46**:654

[21] Ederer C, Spaldin NA. Effect of epitaxial strain on the spontaneous polarization of thin film ferroelectrics. Physical Review Letters. 2005;**95**(25):257601

[22] Cheng CJ, Lu CL, Chen ZH, You L, Chen L, Wang J, Wu T. Thickness-dependent magnetism and spin-glass behaviors in compressively strained $BiFeO_3$ thin films. Applied Physics Letters. 2011;**98**(24):242502

[23] Zhang JX, He Q, Trassin M, Luo W, Yi D, Rossell MD, Yu P, You L, Wang CH, Kuo CY, Heron JT, Hu Z, Zeches RJ, Lin HJ, Tanaka A, Chen CT, Tjeng LH, Chu YH, Ramesh R. Microscopic origin of the giant ferroelectric polarization in tetragonal-like $BiFeO_3$. Physical Review Letters. 2011;**107**(14):147602

[24] Chen ZH, Zou X, Ren W, You L, Huang CW, Yang YR, Yang P, Wang JL. Study of strain effect on in-plane polarization in epitaxial BiFeO3 thin films using planar electrodes. Physical Review B. 2012;**86**:235125

[25] Chen P, Podraza NJ, Xu XS, Melville A, Vlahos E, Gopalan V, Ramesh R, Schlom DG, Musfeldt JL. Optical properties of quasi-tetragonal $BiFeO_3$ thin films. Applied Physics Letters. 2010;**96**:131907

[26] Sturman BI, Fridkin VM. The Photovoltaic and Photorefractive Effects in Noncentrosymmetric Materials. Gordon and Breach Science; 1992

[27] Ji W, Yao K, Liang YC. Evidence of bulk photovoltaic effect and large tensor coefficient in ferroelectric $BiFeO_3$ thin films. Physical Review B. 2011;**84**:094115

[28] Festl HG, Hertel P, Kratzig E, von Baltz R. Investigations of the Photovoltaic Tensor in Doped $LiNbO_3$. Physica Status Solidi (B). 1982;**113**:157-164